Universiteit Antwerpen

This item is the archived peer-reviewed author-version of:

Twin-jet electropolishing for damage-free transmission electron microscopy specimen preparation of metallic microwires

Reference:
Pourbabak Saeid, Orekhov Andrey, Schryvers Dominique.- Twin-jet electropolishing for damage-free transmission electron microscopy specimen preparation of metallic microwires
Microscopy research and technique - ISSN 1059-910X - Hoboken, Wiley, 84:2(2020), p. 298-304
Full text (Publisher's DOI): https://doi.org/10.1002/JEMT.23588
To cite this reference: https://hdl.handle.net/10067/1719690151162165141

uantwerpen.be
Institutional repository IRUA

Twin–jet electropolishing for damage–free TEM specimen preparation of metallic microwires

Running head: Twin–jet electropolishing of microwires

Saeid Pourbabak (saeid.pourbabak@uantwerpen.be, corresponding author)
Andrey Orekhov (andrey.orekhov@uantwerpen.be)
Dominique Schryvers (nick.schryvers@uantwerpen.be)

EMAT, University of Antwerp, Groenenborgerlaan 171, B–2020 Antwerp, Belgium

A method to prepare TEM specimens from metallic microwires and based on conventional twin–jet electropolishing is introduced. The wire is embedded in an opaque epoxy resin medium and the hardened resin is mechanically polished to reveal the wire on both sides. The resin containing wire is then cut into discs of the appropriate size. The obtained embedded wire is electropolished in a conventional twin–jet electropolishing machine until electron transparency in large areas without radiation damage is achieved.

Keywords: TEM specimen preparation, Twin–jet electropolishing, NiTi, Undersized samples, Microwires

Highlights:

- Electropolishing of NiTi microwires is developed
- Wide and damage-free electron transparent area is obtained
- 80% success rate is achieved

1 Introduction

The necessity for this work became apparent during transmission electron microscopy (TEM) investigations of shape memory $Ni_{50.8}Ti_{49.2}$ microwires with a diameter of 150 µm (Pourbabak et al., 2020). Due to the small diameter of these wires, cross–sectional focused ion beam (FIB) sample preparation seemed to be the most appropriate thinning procedure. However, FIB induced damages such as dislocation loops (Samaeeaghmiyoni et al., 2017) severely hamper, e.g., a proper interpretation of high resolution images, needed in a study of nano–precipitates and diffuse intensities (Pourbabak et al., 2017) of quenched solution–treated samples. Moreover, the ~5×10 μm^2 dimensions of a typical FIB specimen would require mechanical polishing of the wire to reach a specific location but which introduced dislocations beneath the surface and that are still visible in the FIB samples (see supplementary info). Also, the FIB sample size does not allow proper statistical investigations in real nor reciprocal space, which appeared necessary in the above-mentioned study. Therefore, the use of conventional electropolishing for obtaining thin TEM samples with large electron transparent areas was reconsidered.

Electropolishing for TEM sample preparation initially proposed by Heidenreich in 1949 for aluminum and aluminum–copper (Heidenreich, 1949) and later extended with a twin–jet modification (Booker & Stickler, 1962; Hugo & Phillips, 1963, 1965; Schoone & Fischione, 1966) is one of the cheapest, fastest and cleanest methods to prepare TEM specimens from bulk electrically conductive materials such as metals and alloys. In this method the material is electrochemically removed from both sides of a mechanically thinned disc of, e.g., 3 mm diameter and 100 µm – 150 µm thick, until sample perforation occurs. The surroundings of the small perforation are sufficiently thin for TEM. The achieved specimen is free of mechanical or ion damage, typically shows large regions of electron transparent material, requires no grid to be mounted on the TEM holder and is easy to handle due to the rigid rim which supports and protects the thin area in the center (Heidenreich, 1949; Wilhelm, 1964). Also heating of the specimen by the electron beam during TEM investigations remains limited since the heat generated in the thin region is rapidly dissipated by the rather thick surroundings (Van Torne & Thomas, 1965). Electropolishing is specifically appropriate for (inter)metallic samples, since these materials are too soft for crushing and easily damaged or altered by ion milling (Bals et al., 2007; Thompson et al., 2019; Knipling et al., 2010; Unocic et al., 2010; Zelaya & Schryvers, 2011). However, the conventional twin–jet electropolishing apparatuses are designed for bulk material from which discs of 3 or 2.3 mm diameter can be obtained and can normally not be applied for specimens of smaller size such as microwires.

Very few studies have been performed on TEM specimen electropolishing of samples smaller than the conventional 3 or 2.3 mm discs. Stickler & Engle (Stickler & Engle, 1963) electropolished 1 mm diameter wires of tungsten and bismuth telluride in a two–step procedure of indentation and thinning of the center of the wire which is not practical for wires thinner than 1 mm. Kestel (Kestel, 1990) introduced three methods in which small sized samples were plated, attached or embedded with a surrounding metal yielding a 3 mm disc. The idea of enlarging the sample to a 3 mm size

was retained in the present work, but due to the further reduction of the size of the original material, an alternative approach had to be introduced which does not have the disadvantage of manipulating the specimen at high temperature or contaminating it with other metals, as is unavoidable in the Kestel procedure. The concept of this work is shown using the above–mentioned Ni–Ti microwires but is applicable to every metallic microwire of similar size when adapting the electrochemical thinning conditions (chemical solution, voltage, temperature, …) appropriate for the respective material.

2 Material and methods

Electropolishing of bulk Ni–Ti for TEM specimen preparation has been widely and commonly applied since 1971 (Nagasawa, 1971). Three main electrolyte solutions have been used for Ni–Ti electropolishing, each with its own pros and cons:

1. Mixture of ~20% sulfuric acid and ~80% methanol is best for materials close to equiatomic Ni–Ti, but in case of existence of Ni_4Ti_3 precipitates, the latter are preferentially thinned (Bals et al., 2007).
2. Mixture of ~93% acetic acid and ~7% perchloric acid gives poorer results overall, but shows no preferential etching between possible precipitates and matrix (Tirry & Schryvers, 2005).
3. Mixture of ~30% nitric acid and ~70% methanol, which should be used with care since at the recommended working temperature (~-30 °C) Ni–Ti with higher Ni–content might undergo a martensitic transformation during polishing.

The current microwires under investigation are in the B2 phase at room temperature and do not contain any full–grown Ni_4Ti_3 precipitates and thus the mixture of 20% sulfuric acid in 80% methanol operating at 18 V (0.13 A) and 0 °C was used.

3 Results

3.1 Designed procedure

The main idea is to embed the microwire under consideration in a medium in such a way that 1) the obtained complex fits into the clamping holder of a twin–jet electropolishing unit, which means having a disc shape of 3 mm diameter and ~150 μm thickness, and 2) the wire is exposed on both sides of the embedding disc so that it can be reached by the electrolyte during the process.

To be applicable for this purpose the embedding medium should have the following properties:

1. Being adhesive, so that it can embed the wire, and being hard enough after hardening, so that it can endure the mechanical stress due to the mechanopolishing without cracking and detaching from the wire.

2. Resistant to the applied electropolishing electrolyte (acids + alcohols), e.g., sulfuric acid and methanol which are used in this work.
3. Resistant to acetone, which is used to remove the glue from the medium in the mechanopolishing procedure.
4. Being electrically conductive to establish electrical contact between the embedded wire and the electropolisher holder.
5. Being non–transparent, so that it can block the light–photocell path in the unit and allow the use of the automated stop mechanism of the setup.

Epoxy resins are found to match the three first conditions since they suffer least from chemical attack and show true adherence to the sample, especially metals (Samuels, 2003). They induce no chemical reaction with the material and cause no contamination on the material surface. However, epoxy resins with no filler are generally semitransparent and non–conductive, so some kind of filler needs to be used in order to match conditions 4 and 5.

Electrically conductive epoxies and that are non–transparent due to a filler content are commercially available, however, the vast majority of these are silver–filled, some other copper–, nickel– and gold–filled, which all dissolve in the sulfuric acid mixture under the present electropolishing conditions (Lyles et al., 1978; Toušek, 1977; Wolf, 1977). Very few epoxy resins with graphite as filler and which do not react with acids exist. Moreover, they all share the disadvantage of having a resistivity of orders of magnitude higher than that of the metal–filled resins, which hampers electropolishing. For example, the volume resistivity of the graphite–filled EPO–TEK 377H (*Product Detail EPO-TEK 377H*, n.d.) epoxy resin is more than 400 Ω.cm, while that of the silver–filled EPO–TEK H20E (*Product Detail EPO-TEK H20E*, n.d.) is less than 0.0004 Ω.cm. For this reason, placing the wire perpendicular to the disc surface, as shown in Figure 1 (a) and needed when the cross–section TEM view of an, e.g., textured wire is desired, and relying on the resin conductivity to make electrical contact between the wire and the platinum strip of the holder does not lead to proper electropolishing, but partial etching instead. In Figure 2 an example of such an experiment with graphite–filled EPO–TEK 377H is shown under a light optical microscope (Figure 2 (a)) and BF–TEM (Figure 2 (b) and (c)). It can be seen from the SAED in Figure 2 (d) that some electron transparent regions are indeed obtained, but the specimen thickness is not uniform and the surface is rough (due to partial etching). These results suggest that the perpendicular method can only be successful if a high conductive epoxy resin is applied, but the available systems, e.g., silver–filled EPO–TEK H20E, would dissolve in our chemical mixture.

In order to avoid this conflict of needed properties for the embedding medium, the electric contact can be obtained by embedding the wire in the resin parallel to the surface of the 3 mm disc (Figure 1 (b)) and ensuring direct electrical contact between the wire and the metallic strip of the holder. The length of the wire was thus chosen large enough to reach the platinum of the electropolisher holder on one (or both) sides of the strip hole, as shown in Figure 1 (c), ensuring electrical contact between the sample and the system while the strip also acts as a heat sink minimizing sample heating during polishing. This approach provides a plan–view thinning of the wire sample.

In the present work an EPO–TEK 353ND (*Product Detail EPO-TEK 353ND*, n.d.) epoxy resin was used which is transparent when liquid and becomes amber to dark red after curing. Therefore, complete non–transparency was achieved by adding 10 wt.% graphite powder with particle size of ~5 μm to the resin. This amount of graphite makes the resin non–transparent but has no effect on the electrical conductivity. Mixing the epoxy, the hardener and the graphite powder should be done gently to avoid forming tiny bubbles. In case of micro–bubbles formation in the resin, vacuum degassing or centrifuging should be carried out to eliminate minute air bubbles and prevent the appearance of holes in the final polished resin disc.

The standard Tenupol holders for 3 and 2.3 mm samples have a platinum strip hole of diameter 2.6 and 2.1 mm, respectively. The latter is used for this work since it allows the use of shorter wires. Since it is sufficient for the wire to be in contact with the platinum strip only on one side, there is no need for the wire to be longer than 2.1 mm. It only needs to be placed in the resin disc in such a way that when mounting in the electropolisher holder 1) the wire is connected to at least one side of the strip hole, 2) the wire reaches the center of the hole where the electrolyte jet is most active, and 3) the resin disc completely blocks the holder hole, as shown in Figure 1 (c).

The wires were chopped into a length of ~2 mm and placed on a microscope glass slide wrapped in Teflon tape which eases detaching of the resin after hardening, as shown in S1 supplementary video. A drop of resin mixture was placed on each wire piece using a needle (see supplementary S2 video). The resin drop should be big enough to make a hemisphere with a diameter of appr. 3 mm, completely covering the wire, as schematically shown in Figure 3 (a). Due to the still viscous nature of the resin some resin will flow underneath the wire, but most of the resin will form the hemisphere above the wire. The resin was then left to harden at room temperature which took about 4 days. In case the sample is not affected at elevated temperature, the resin can be heated up to speed up hardening according to the resin technical data sheet, e.g., 10 minutes at 100 °C. An image of hardened hemisphere resins is shown in Figure 3 (b).

The hardness of the resin was checked by scratching the surface with a sharp needle. Then it was mechanopolished from both sides until a disc of ~100 μm thickness was obtained with the wire surface appearing from both sides of the disc. To this purpose the resin embedding the wires was fixed on a microscope slide to be held and handled easily using Crystalbond™ 821–3 adhesive which melts at ~120 °C, requiring a few seconds heating at each attaching or detaching step. Polishing should start from coarse to soft paper, each step removing the plastically deformed or structurally altered layers induced by the previous polishing step. As a rule of thumb, polishing with abrasive papers can produce a depth of damage to the material up to three times the size of the abrasive particles (Ayache et al., 2010). The polishing steps should be carried out in a way that after the last polishing the sample is slightly thicker than twice the damage penetration depth of the last polishing step so that the central part of the material is unaffected (Thompson-Russell & Edington, 1977). After achieving the final thickness, the disc should be rinsed in acetone to completely remove the remaining adhesive. An image of some mechanopolished discs is shown in Figure 3 (c).

As from this point the resin disc embedding the wire should be handled gently since it is fragile. When possible, using a vacuum pickup tool instead of tweezers is recommended for picking up the disc.

If the resin disc is larger than 3 mm, it should be resized to fit into the TEM holder. To this purpose the resin disc perimeter is cut using a scalpel. In order to minimize the risk of breaking the resin disc or detaching the wire from it, cutting should be done by pressing a curved scalpel down from one side of the resin disc to another with a rolling movement over the curved edge of the blade, instead of pulling the blade in a horizontal direction, or landing it in the vertical direction, as shown in S3 supplementary material. A resin disc before cutting and another after cutting are shown in Figure 4 (a).

The disc was mounted into the twin–jet electropolisher holder in the way that the wire connects to the edge of the hole of the platinum strip of the holder, as was shown in Figure 1 (c). The holder is then inserted into the electropolisher, settings of the machine are set equal to those of the respective bulk material, and the electropolishing procedure can be started.

Voltage and current indicators of the electropolisher control unit give information about the process and whether or not electropolishing is occurring. When both potential and current are non–zero, electrolytic action occurs. If the potential is non–zero but the current is zero, the electrical contact between the wire sample and the apparatus is not established (Luo, 2015). If both potential and current are zero, this is an indication that the auto–stop has been triggered even before electropolishing starts. This might happen for the present resin embedded wire samples due to the semi–transparency of the thin filled resin. In bulk Ni–Ti the material completely blocks the light source–photocell path and photosensitivity determines the perforation size. In the resin embedded wire disc, however, the graphite–filled resin can transmit some light when thinned to around 100 μm. Therefore, the light received by the photocell is a combination of wire perforation and transmitted light through the resin. As the resin disc thickness and graphite content or distribution might be slightly different from one sample to another, the photosensitivity should be adjusted as follows: it is set to 8, as for bulk material. If the current and potential are both zero, which means the auto–stop mechanism is activated, photosensitivity is set to zero and the start button is pushed again. Then the photosensitivity is increased until the auto–stop is triggered due to the semi–transparency of the resin, so the photosensitivity number in which the auto–stop is activated is found. Then electropolishing is restarted with the photosensitivity set to a number ~0.5–1 lower than the triggering number. With judicious adjustments of the photosensitivity a successful electropolished specimen can be obtained and the procedure has a success yield of around 80%.

The achieved specimen is examined after rinsing and drying. As the wire is already thinned, even if the resin breaks at this step, the specimen can still be used, as shown in Figure 4 (b).

When mounting the specimen in the TEM holder the wire should be in contact with the holder to avoid charge accumulation on the specimen. In case this is not possible due to size limitations of the wire, a 5 nm carbon layer can be deposited on the surface of the resin.

3.2 Sample quality

A light optical microscope (LOM) image of a Ni–Ti microwire TEM specimen obtained by the above method is shown in Figure 5 (a). In this image the perforation in the center of the wire is clearly seen. The corresponding low magnification scanning TEM (LM–STEM) image is shown in Figure 5 (b). A higher magnification bright field (BF) TEM image is presented in Figure 5 (c) together with a selected area electron diffraction pattern (SAED) as inset. In Figure 5 (d) a high resolution (HR)–STEM image along the $\langle 111 \rangle_{B2}$ direction is presented. The BF TEM image, the diffraction pattern as well as the HR–STEM showing atomic resolution clearly indicate the local quality of the thinning procedure. The grains in Figure 5 (c) do not contain any thinning induced defects, the thickness allows for the observation of diffuse intensity in the SAED inset and referring to local ordering (Pourbabak et al., 2017) and the high resolution in Figure 5 (d) reveals a perfect lattice from which the lack of precipitation could be concluded. No extra reflections due to any hydrogen interstitial ordering after electropolishing as reported in earlier studies (Nishida et al., 1993; Wu & Wayman, 1988) were observed, possibly because the samples were only investigated a day after the electropolishing allowing the hydrogen to diffuse out of the sample. The LM–STEM image in Figure 5 (b) reveals a successful thinning not only at a single site but around the entire hole.

In another specimen two major and elongated holes appeared along the wire, shown in Figure 6 (a) inset, providing thin areas between the holes in addition to the surroundings. A LM–STEM image of the region between the two holes is shown in Figure 6 (a). In Figure 6 (b) an ADF image of the white rectangle indicated in Figure 6 (a) is shown with the corresponding electron energy loss spectroscopy (EELS) thickness map in Figure 6 (c) (Leapman et al., 1984; Malis et al., 1988). The thickness map shows that the sample thickness reaches about 20 nm – 25 nm in the thinnest region. It also reveals that a 2 μm –3 μm wide band with a thickness lower than 50 nm surrounds the holes and reaches a width up to 5 μm between the holes, yielding a total area of 350 μm^2, much larger than what is obtained with conventional FIB samples (typically 5×10 μm^2) and useful for statistical investigations such as texture analysis.

In Figure 6 (d)–(e) the results of an automated crystal orientation mapping (ACOM)–TEM experiment on the red rectangle between the two perforations in Figure 6 (a) are presented. Figure 6 (d), the orientation map, shows the sub–micron size grains in the thinned region, while the top and bottom of the map is noisy due to the higher thickness of the sample at those areas far from the perforation. In the center of the image, on the other hand, the same is true for the highly strained region due to the very thin thickness and vicinity of the crack. In Figure 6 (e) five nano–beam diffraction patterns selected from the indicated spots of Figure 6 (c) confirm the quality of thinning for the central grains. All of the examples shown in Figures 5 and 6 proof that this sample

preparation method can be used to obtain useful data of various types from metallic microwires without the need for (focused) ion milling introducing various kinds of radiation damage in the sample.

4 Conclusions

A novel method to prepare TEM specimens from metallic microsize thin wires is introduced and which can be used with instrumentation available in most of the materials science electron microscopy laboratories. The handled object is enlarged in size by embedding the wire into a filled resin medium after which it is treated as bulk material and electropolished by a conventional twin–jet electropolishing apparatus. The result is a well–polished specimen without radiation damage and large polished areas perfectly suited for conventional as well as advanced TEM investigations and with a success rate similar to that of bulk material.

5 Acknowledgements

S.P. and A.O. like to thank the Flemish Science Foundation FWO for financial support under Project G.0366.15N.

6 References

Ayache, J., Beaunier, L., Boumendil, J., Ehret, G., & Laub, D. (2010). *Sample Preparation Handbook for Transmission Electron Microscopy: Techniques*. Springer-Verlag. //www.springer.com/gp/book/9781441959744

Bals, S., Tirry, W., Geurts, R., Yang, Z., & Schryvers, D. (2007). High-quality sample preparation by low kV FIB thinning for analytical TEM measurements. *Microscopy and Microanalysis: The Official Journal of Microscopy Society of America, Microbeam Analysis Society, Microscopical Society of Canada*, *13*(2), 80–86. https://doi.org/10.1017/S1431927607070018

Booker, G. R., & Stickler, R. (1962). Method of preparing Si and Ge specimens for examination by transmission electron microscopy. *British Journal of Applied Physics*, *13*(9), 446. https://doi.org/10.1088/0508-3443/13/9/303

Heidenreich, R. D. (1949). Electron Microscope and Diffraction Study of Metal Crystal Textures by Means of Thin Sections. *Journal of Applied Physics*, *20*(10), 993–1010. https://doi.org/10.1063/1.1698264

Hugo, J. A., & Phillips, V. A. (1963). A versatile jet technique for thinning metals for transmission electron microscopy. *Journal of Scientific Instruments*, *40*(4), 202. https://doi.org/10.1088/0950-7671/40/4/427

Hugo, J. A., & Phillips, V. A. (1965). A twin-jet technique for thinning metals for transmission electron microscopy. *Journal of Scientific Instruments*, *42*, 354–355.

Kestel, B. J. (1990). Improved Methods and Novel Techniques for Jet Electropolishing of TEM Foils*. *MRS Online Proceedings Library Archive*, *199*. https://doi.org/10.1557/PROC-199-51

Knipling, K. E., Rowenhorst, D. J., Fonda, R. W., & Spanos, G. (2010). Effects of focused ion beam milling on austenite stability in ferrous alloys. *Materials Characterization*, *61*(1), 1–6. https://doi.org/10.1016/j.matchar.2009.09.013

Leapman, R. D., Fiori, C. E., & Swyt, C. R. (1984). Mass thickness determination by electron energy loss for quantitative X-ray microanalysis in biology. *Journal of Microscopy*, *133*(3), 239–253. https://doi.org/10.1111/j.1365-2818.1984.tb00489.x

Luo, Z. (2015). *Practical Guide to Transmission Electron Microscopy.* Momentum Press. http://www.myilibrary.com?id=875795

Lyles, R. L., Rothman, S. J., & Jäger, W. (1978). A cyanide-free solution for electropolishing silver. *Metallography*, *11*(3), 361–363. https://doi.org/10.1016/0026-0800(78)90049-6

Malis, T., Cheng, S. C., & Egerton, R. F. (1988). EELS log-ratio technique for specimen-thickness measurement in the TEM. *Journal of Electron Microscopy Technique*, *8*(2), 193–200. https://doi.org/10.1002/jemt.1060080206

Nagasawa, A. (1971). Martensite Transformation and Memory Effect in the NiTi Alloy. *Journal of the Physical Society of Japan*, *31*(1), 136–147. https://doi.org/10.1143/JPSJ.31.136

Nishida, M., Yamauchi, K., Chiba, A., & Higashi, Y. (1993). Internal structure of triangular self-accommodating martensite in Ti-Ni shape memory alloy. *Proceedings of the International Conference on Martensitic Transformations (ICOMAT-92)*, 881–886.

Pourbabak, S., Verlinden, B., Van Humbeeck, J., & Schryvers, D. (2020). DSC Cycling Effects on Phase Transformation Temperatures of Micron and Submicron Grain Ni50.8Ti49.2 Microwires. *Shape Memory and Superelasticity*. https://doi.org/10.1007/s40830-020-00278-y

Pourbabak, S., Wang, X., van Dyck, D., Verlinden, B., & Schryvers, D. (2017). Ni cluster formation in low temperature annealed Ni50.6Ti49.4. *Functional Materials Letters*, *10*, 1740005. https://doi.org/10.1142/S1793604717400057

Product Detail EPO-TEK 353ND. (n.d.). Epoxy Technology. Retrieved June 7, 2019, from https://www.epotek.com/site/component/products/productdetail.html?cid[0]=29

Product Detail EPO-TEK 377H. (n.d.). Epoxy Technology. Retrieved June 7, 2019, from https://www.epotek.com/site/component/products/productdetail.html?cid[0]=39

Product Detail EPO-TEK H20E. (n.d.). Epoxy Technology. Retrieved June 7, 2019, from https://www.epotek.com/site/component/products/productdetail.html?cid[0]=84

Samaeeaghmiyoni, V., Idrissi, H., Groten, J., Schwaiger, R., & Schryvers, D. (2017). Quantitative in-situ TEM nanotensile testing of single crystal Ni facilitated by a new

sample preparation approach. *Micron*, *94*, 66–73. https://doi.org/10.1016/j.micron.2016.12.005

Samuels, L. E. (2003). *Metallographic polishing by mechanical methods*. ASM International. http://public.eblib.com/choice/publicfullrecord.aspx?p=3002435

Schoone, R. D., & Fischione, E. A. (1966). Automatic Unit for Thinning Transmission Electron Microscopy Specimens of Metals. *Review of Scientific Instruments*, *37*(10), 1351–1353. https://doi.org/10.1063/1.1719978

Stickler, R., & Engle, R. J. (1963). Microjet method for preparation of wire samples for transmission electron microscopy. *Journal of Scientific Instruments*, *40*(11), 518. https://doi.org/10.1088/0950-7671/40/11/303

Thompson, A. W., Harris, Z. D., & Burns, J. T. (2019). Examination of focused ion beam-induced damage during platinum deposition in the near-surface region of an aerospace aluminum alloy. *Micron*, *118*, 43–49. https://doi.org/10.1016/j.micron.2018.12.004

Thompson-Russell, K. C., & Edington, J. W. (1977). Electron Microscope Specimen Preparation Techniques in materials Science. In K. C. Thompson-Russell & J. W. Edington (Eds.), *Electron Microscope Specimen Preparation Techniques in Materials Science* (pp. 1–136). Macmillan Education UK. https://doi.org/10.1007/978-1-349-03403-1_1

Tirry, W., & Schryvers, D. (2005). Quantitative determination of strain fields around Ni4Ti3 precipitates in NiTi. *Acta Materialia*, *53*(4), 1041–1049. https://doi.org/10.1016/j.actamat.2004.10.049

Toušek, J. (1977). Electropolishing of metals in alcoholic solution of sulphuric acid. *Electrochimica Acta*, *22*(1), 47–50. https://doi.org/10.1016/0013-4686(77)85052-4

Unocic, K. A., Mills, M. J., & Daehn, G. S. (2010). Effect of gallium focused ion beam milling on preparation of aluminium thin foils. *Journal of Microscopy*, *240*(3), 227–238. https://doi.org/10.1111/j.1365-2818.2010.03401.x

Van Torne, L. I., & Thomas, G. (1965). Micro-Electropolishing Transmission Electron Microscopy Specimens. *Review of Scientific Instruments*, *36*(7), 1042–1043. https://doi.org/10.1063/1.1719756

Wilhelm, F. J. (1964). The preparation of beryllium specimens for transmission electron microscopy by the Knuth system of electropolishing. *Journal of Scientific Instruments*, *41*(5), 343. https://doi.org/10.1088/0950-7671/41/5/439

Wolf, R. (1977). Electropolishing of gold and gold-rich alloys. *Micron (1969)*, *8*(3), 171–172. https://doi.org/10.1016/0047-7206(77)90021-8

Wu, S. K., & Wayman, C. M. (1988). Interstitial ordering of hydrogen and oxygen in TiNi alloys. *Acta Metallurgica*, *36*(4), 1005–1013. https://doi.org/10.1016/0001-6160(88)90155-1

Zelaya, E., & Schryvers, D. (2011). Reducing the formation of FIB-induced FCC layers on Cu-Zn-Al austenite. *Microscopy Research and Technique*, *74*(1), 84–91. https://doi.org/10.1002/jemt.20877

Figure legends:

Figure 1 Wire piece embedded (a) perpendicular and (b) parallel to the disc surface. (c) Schematic of a resin disc embedding a 1.9 mm long wire piece overlaid on a platinum hole of a Tenupol holder, connecting to the platinum on the right side.

Figure 2 (a) Low magnification light optical microscope and (b) BF–TEM image of three perpendicularly embedded electropolished micro–wires, (c) higher magnification BF–TEM image of the edge of one of wires showing non–uniform thinning, (d) SAED of the same region.

Figure 3 (a) Schematic of the wire embedded into a hemisphere resin, (b) hardened hemisphere resin containing wires, (c) mechanopolished discs.

Figure 4 (a) Left to right, a 3 mm cupper grid as reference size, a resin disc larger than 3 mm diameter and another resin disc after being cut, (b) a sample with the resin half–disc broken and detached from the wire after electropolishing and cutting, but still usable when mounted in a TEM holder.

Figure 5 (a) LOM image of the specimen after electropolishing showing the perforation in the wire, (b) LM–STEM image of the specimen shown in a, (c) a BF–TEM image of some grains of the wire together with the SAED pattern (inset), (d) HR–STEM image with the corresponding fast Fourier transformation (inset).

Figure 6 (a) LM–STEM image of a specimen where two lateral elongated holes meet with the LOM inset showing the elongated holes, (b) higher magnification ADF image of the white rectangle region indicated in (a), showing a crack in the middle, (c) EELS color coded thickness map of (b) in nanometer, (d) orientation map obtained from the nano–beam scanning of the red rectangle area between the two holes of (a), (e) nano–beam diffraction of the indicated spots of (d), revealing the thickness dependency of the number of distinguishable diffracted spots.

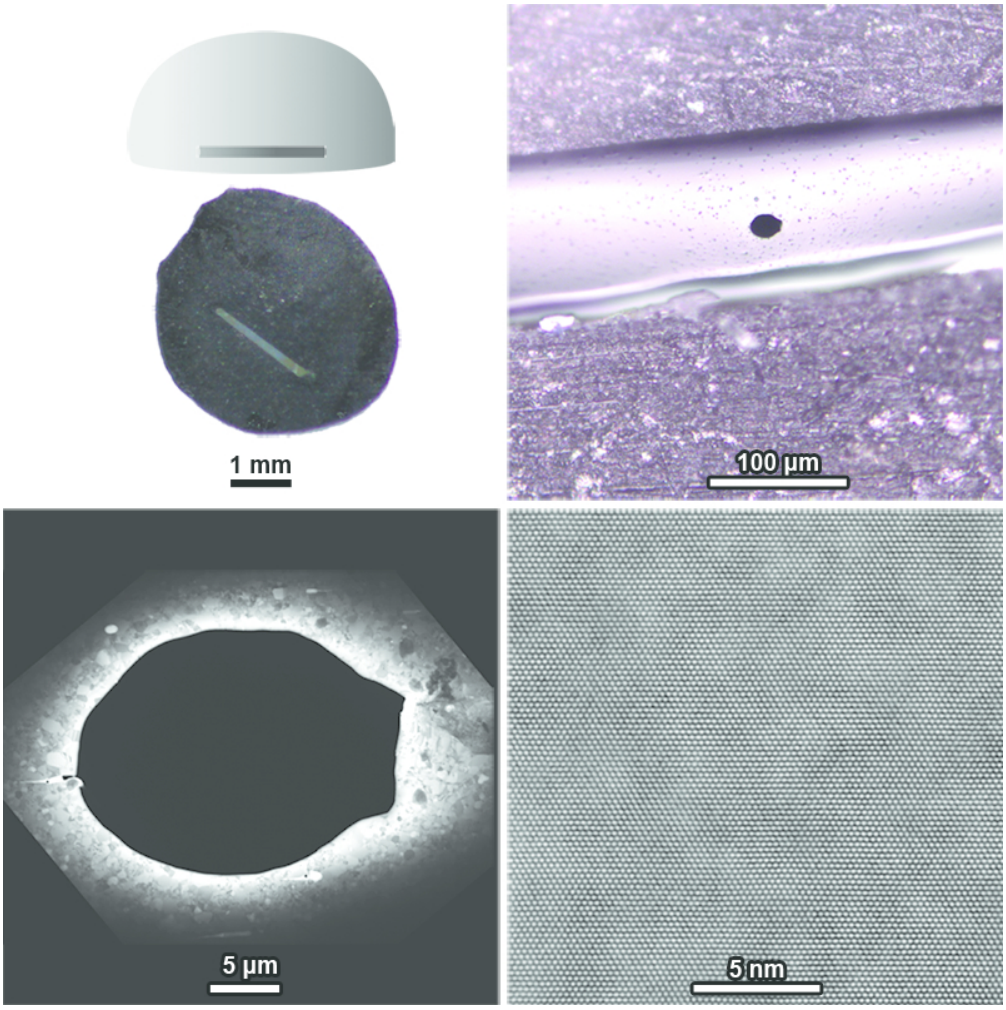

Graphical Abstract

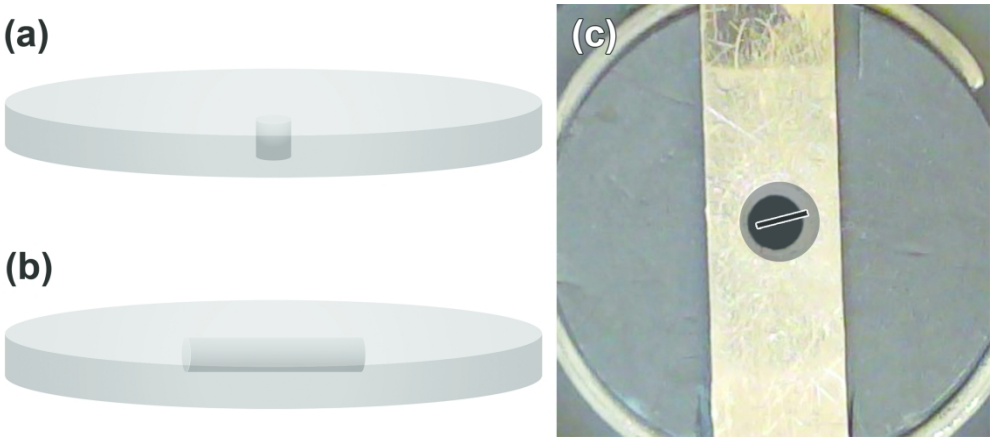

Figure 1 Wire piece embedded (a) perpendicular and (b) parallel to the disc surface. (c) Schematic of a resin disc embedding a 1.9 mm long wire piece overlaid on a platinum hole of a Tenupol holder, connecting to the platinum on the right side.

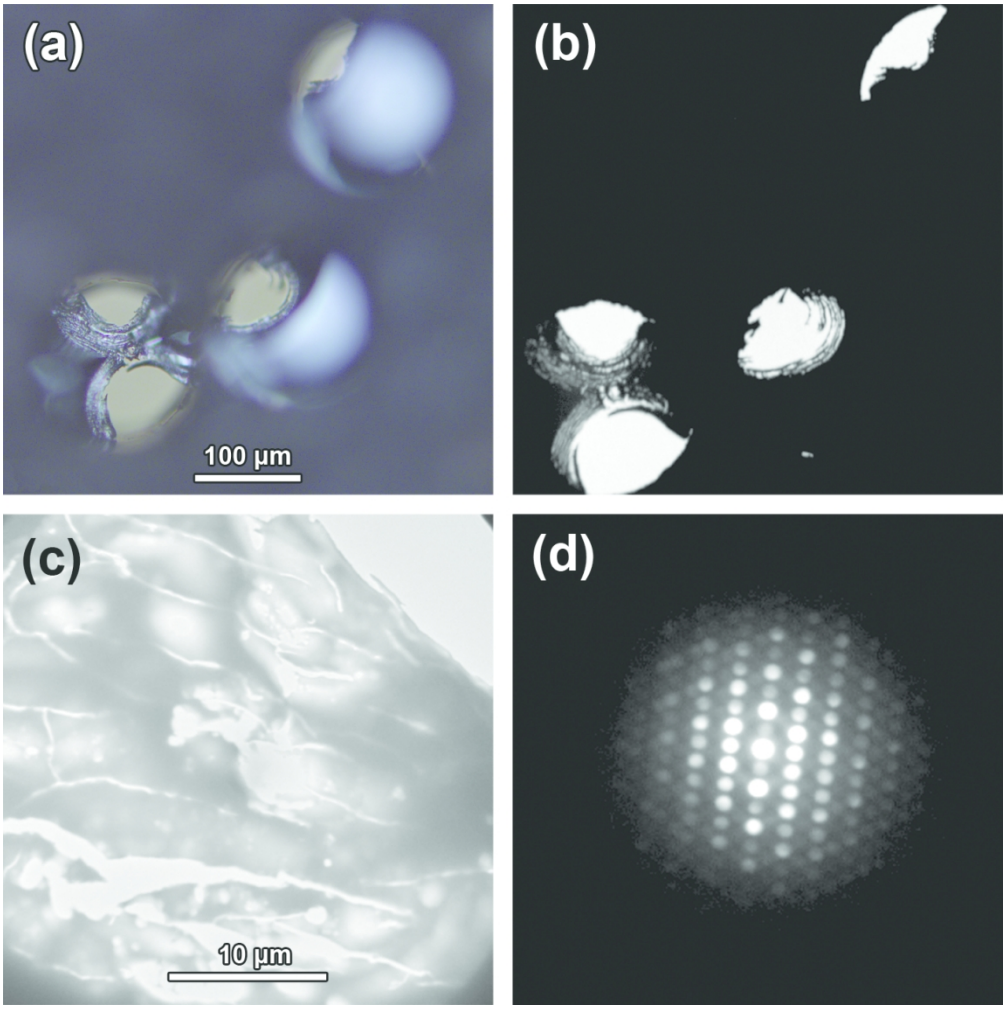

Figure 2 (a) Low magnification light optical microscope and (b) BF–TEM image of three perpendicularly embedded electropolished micro–wires, (c) higher magnification BF–TEM image of the edge of one of wires showing non–uniform thinning, (d) SAED of the same region.

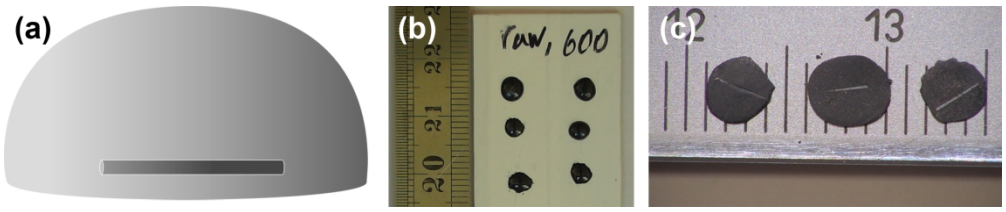

Figure 3 (a) Schematic of the wire embedded into a hemisphere resin, (b) hardened hemisphere resin containing wires, (c) mechanopolished discs.

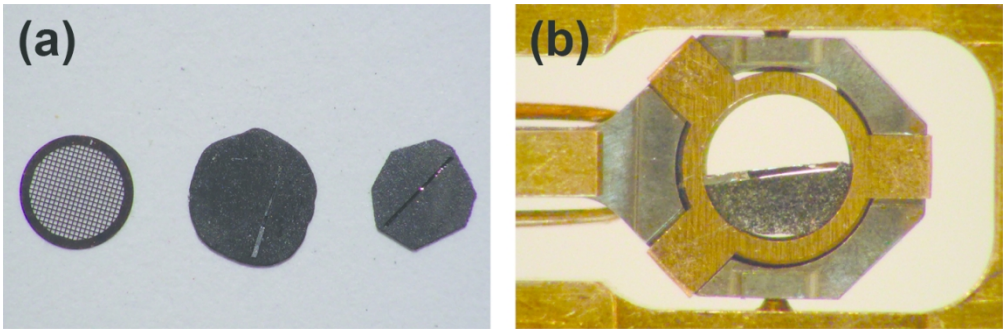

Figure 4 (a) Left to right, a 3 mm cupper grid as reference size, a resin disc larger than 3 mm diameter and another resin disc after being cut, (b) a sample with the resin half–disc broken and detached from the wire after electropolishing and cutting, but still usable when mounted in a TEM holder.

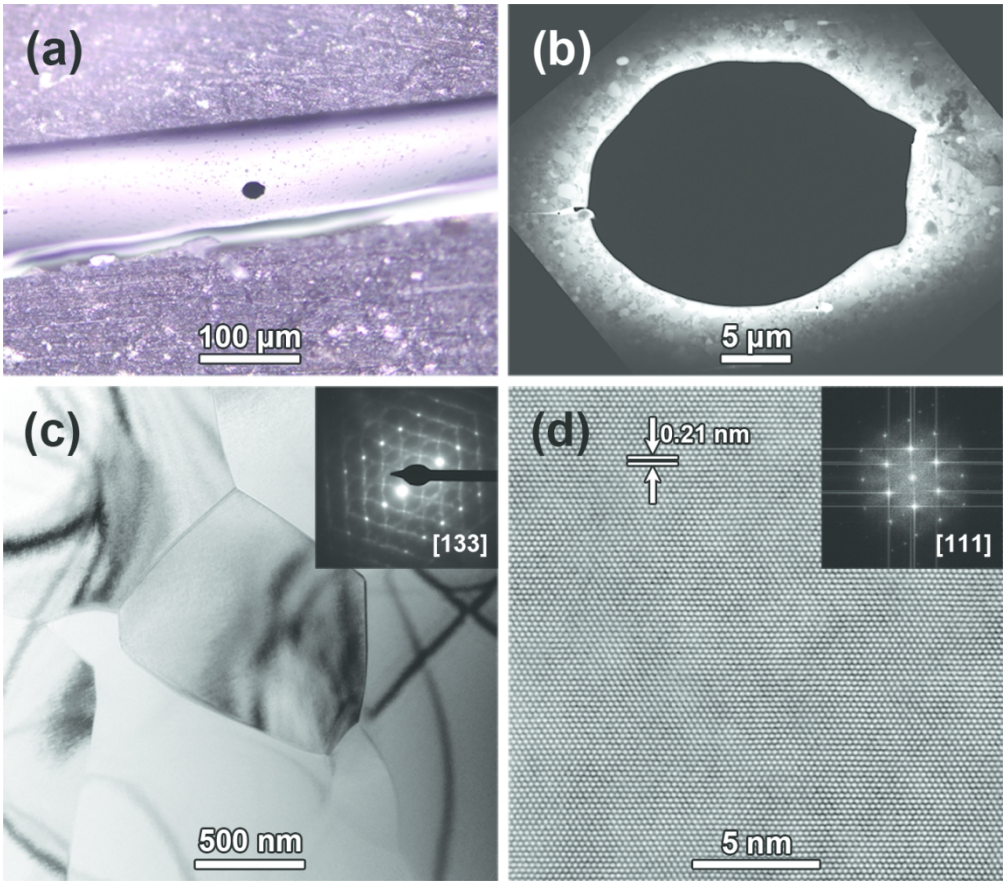

Figure 5 (a) LOM image of the specimen after electropolishing showing the perforation in the wire, (b) LM–STEM image of the specimen shown in a, (c) a BF–TEM image of some grains of the wire together with the SAED pattern (inset), (d) HR–STEM image with the corresponding fast Fourier transformation (inset).

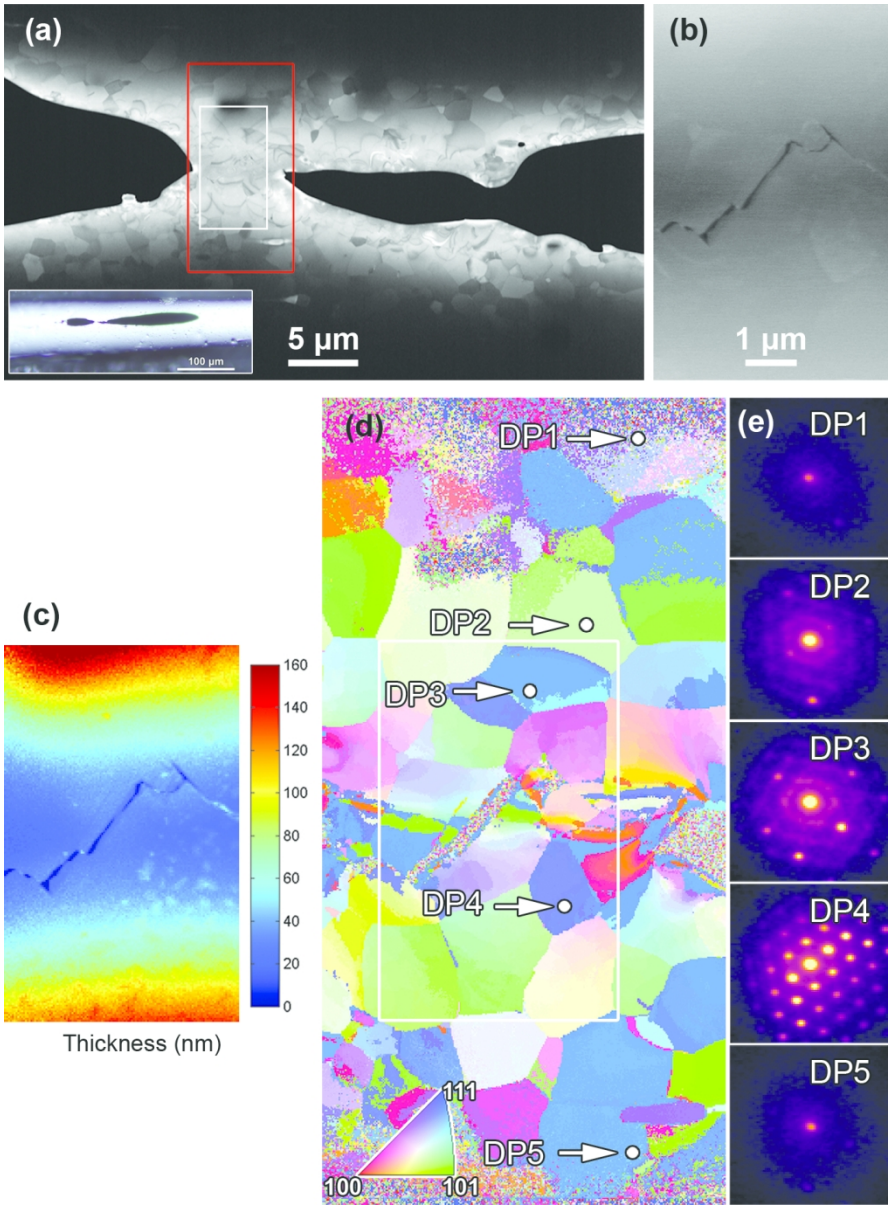

Figure 6 (a) LM–STEM image of a specimen where two lateral elongated holes meet with the LOM inset showing the elongated holes, (b) higher magnification ADF image of the white rectangle region indicated in (a), showing a crack in the middle, (c) EELS color coded thickness map of (b) in nanometer, (d) orientation map obtained from the nano–beam scanning of the red rectangle area between the two holes of (a), (e) nano–beam diffraction of the indicated spots of (d), revealing the thickness dependency of the number of distinguishable diffracted spots.